DOI: 10.1534/genetics.104.026260

A Role for DNA Polymerase δ in Gene Conversion and Crossing Over During Meiosis in *Saccharomyces cerevisiae*

Laurent Maloisel,*,[1] Jaya Bhargava[†,2] and G. Shirleen Roeder*,[†,‡,3]

**Howard Hughes Medical Institute, [†]Department of Molecular, Cellular and Developmental Biology and [‡]Department of Genetics, Yale University, New Haven, Connecticut 06520-8103*

Manuscript received January 6, 2004
Accepted for publication April 15, 2004

ABSTRACT

A screen for mutants of budding yeast defective in meiotic gene conversion identified a novel allele of the *POL3* gene. *POL3* encodes the catalytic subunit of DNA polymerase δ, an essential DNA polymerase involved in genomic DNA replication. The new allele, *pol3-ct*, specifies a protein missing the last four amino acids. *pol3-ct* shows little or no defect in DNA replication, but displays a reduction in the length of meiotic gene conversion tracts and a decrease in crossing over. We propose a model in which DNA synthesis determines the length of strand exchange intermediates and influences their resolution toward crossing over.

HOMOLOGOUS recombination plays a critical role in maintaining genome integrity throughout cell division. In meiosis, homologous recombination is essential for proper homolog pairing and for the correct segregation of chromosomes at the first meiotic division. In vegetative cells, recombination plays an important role during DNA replication by providing a mechanism to bypass DNA lesions and other obstacles that block replication fork progression. Homologous recombination also provides a means to generate new combinations of genetic markers through gene conversion and crossing over, thereby generating genetic diversity among different individuals in the same population.

Numerous insights into the mechanism of homologous recombination have been obtained from meiotic studies using the convenient model organism, *Saccharomyces cerevisiae* (Paques and Haber 1999). Meiotic recombination in budding yeast is initiated by the formation of DNA double-strand breaks (DSBs) at recombination hotspots. The strands with 5′ ends at the site of the break are processed to expose single-stranded tails with 3′ termini (Figure 1). DSB formation and 5′-end resection are followed by invasion of an intact nonsister chromatid by only one of the two single-stranded tails (Hunter and Kleckner 2001). Single-end invasion results in hybrid DNA (hDNA) in which the two strands in a duplex are of different parental origin. If the two parental duplexes are genetically different within the region of strand exchange, the resulting hDNA contains mismatched base pairs and is referred to as heteroduplex DNA.

Single-end invasion intermediates can be channeled toward either of two repair pathways. In the first pathway, described by the DSB repair model (Szostak *et al.* 1983; Sun *et al.* 1989), DNA synthesis, capture of the second end, and ligation generate a double Holliday junction intermediate with asymmetric hDNA (*i.e.*, hDNA on only one of the two duplexes) on each side of the DSB and on each chromatid (Figure 1, left). If a Holliday junction undergoes branch migration, then hDNA will be formed on both duplexes (symmetric hDNA). Eventually, double Holliday junction intermediates are resolved by cutting, at each junction, either both outside strands or both inside strands. Cutting of the two junctions in opposite directions generates crossovers, while cutting in the same direction generates noncrossovers.

The second pathway is described by the synthesis-dependent strand annealing (SDSA) model (Paques and Haber 1999) and supported by recent meiotic studies (Allers and Lichten 2001; Merker *et al.* 2003). According to the SDSA model (Figure 1, right), the invading strand is extended by DNA synthesis and then subsequently displaced. The newly synthesized DNA strand then anneals to the single-stranded tail on the other side of the break. DSB repair is completed by DNA synthesis and ligation. If extension of the invading strand creates a single-stranded tail that is longer than the exposed complement on the opposite side of the break, a flap structure with an exposed 3′ end will result after the two strands anneal and this flap will need to be removed to allow ligation. In this model, asymmetric hDNA occurs only on one side of the break and only

[1]*Present address:* CEA de Fontenay-aux-Roses, UMR 217 CNRS-CEA/DSV/DRR/LERA, 92265 Fontenay-aux-Roses, France.

[2]*Present address:* End Stage Renal Disease Network of New England, 30 Hazel Terrace, Woodbridge, CT 06525.

[3]*Corresponding author:* Howard Hughes Medical Institute, Department of Molecular, Cellular and Developmental Biology, Yale University, P.O. Box 208103, New Haven, CT 06520-8103.
E-mail: shirleen.roeder@yale.edu

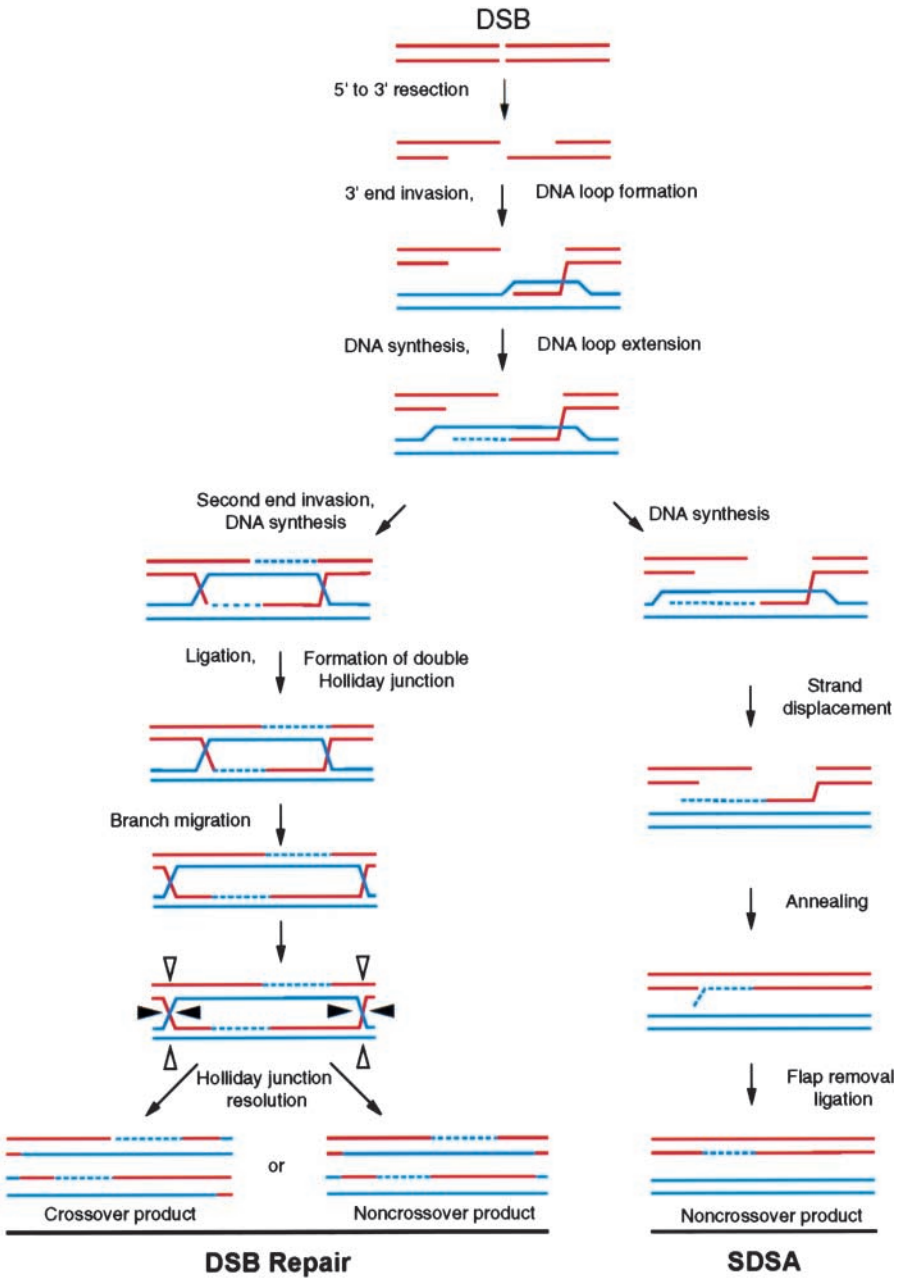

FIGURE 1.—Models of meiotic recombination. Diagrammed are DSB repair by the DSB repair pathway (left) and by SDSA (right). Shown are two recombining DNA duplexes, one indicated in red and the other in blue. See text for details. In the DSB repair model, arrowheads depict cleavage of double Holliday junctions; only two of four possible resolution products are shown.

on the chromatid that suffered the DSB. The SDSA repair pathway does not lead *a priori* to the formation of double Holliday junctions and therefore produces only noncrossover products. Although SDSA is a common mode of DSB repair in vegetative cells (PAQUES and HABER 1999), the extent to which it contributes to meiotic recombination remains unclear.

Although early intermediates in meiotic recombination have been characterized by extensive genetic, biochemical, and physical analyses, the later steps remain obscure. For example, it is not understood what determines the channeling of single-end invasion intermediates into either of the two repair pathways. In the DSB repair pathway, it is not known what controls the elongation of strand exchange intermediates, second-end capture, formation of Holliday junctions, branch migration, or junction resolution. This study provides insight into some of these issues.

We describe a novel allele of the *POL3* gene of *S. cerevisiae* coding for the catalytic subunit of DNA polymerase δ. This mutation has little or no effect on DNA replication or DNA damage repair in vegetative cells. However, during meiotic recombination, the mutant produces shorter strand exchange intermediates and fewer crossover products. These results lead us to propose a role for Polδ in meiotic recombination beyond an involvement in simple gap repair.

MATERIALS AND METHODS

Isolation and mapping of the *pol3-ct* mutant: The *pol3-ct* mutant was isolated using the homothallic (*HO*) strain S2702

(*MAT***a**/*MAT*α and homozygous for *ade2-1 HIS4-ura3-Stu-his4-260 leu2-3,112 lys2-1 thr1-4 trp1-289 ura3-1*). After induction of sporulation and spore enrichment (Rockmill *et al.* 1991) spores were mutagenized with ultraviolet (UV) light to 50% survival and plated on YPD medium. Spore colonies were replica plated to sporulation medium and then to medium lacking uracil to assay the production of uracil prototrophs. The *pol3-ct* mutant was identified on the basis of a strong decrease (~10-fold) in meiotic Ura^+ prototroph formation.

Mapping of the *pol3-ct* mutation was carried out using multiply marked strains (X4119-15D, STX145-15D, STX82-3A, STX153-10C, STX75-3C, STX147-4C, X4120-19D, STX-6C, and STX155-9B) obtained from the Yeast Genetic Stock Center. Strains from our own collection carrying mutations in various meiotic genes (*e.g.*, *MSH5* and *REC102*) were also used.

Strains and plasmids: Strains used to characterize the effect of *pol3-ct* in meiosis are derived from the haploid strains AS4 (*MAT*α *trp1-1 arg4-17 tyr7-1 ade6 ura3 MAL2*) and AS13 (*MAT***a** *leu2-Bst ura3 ade6*) (Nag *et al.* 1989). AS4 is a *HIS4* strain, while the PD strains are *his4* strains derived from AS13 by transformation. PD75 is *his4-ACG* (a T to C transition in the initiating codon), PD5 is *his4-519* (a 1-bp insert at +473), PD22 is *his4-712* (a 1-bp insert at +1396), PD24 is *his4-713* (a 1-bp insert at +2270), and DNY25 is *his4-lopc* (insertion of a palindromic sequence at the *Sal*I site in *HIS4*). *pol3-ct* derivatives of these strains were constructed by the two-step transplacement procedure (Rothstein 1991). In the first step, strains were transformed with *Hin*dIII-digested LMδ1 (see below). Then Ura^- derivatives of Ura^+ transformants were selected on 5-fluoroorotic acid, creating strains LMP6 (AS4), LMP5 (PD75), LMP2 (PD5), LMP3 (PD22), LMP4 (PD24), and LMP8 (DNY25). Replacement of the *POL3* allele by *pol3-ct* was verified by DNA sequencing.

Plasmid GR160 (obtained from Roland Chanet) containing the wild-type *POL3* gene in YCp50 was used to complement the *pol3-ct* defect. The *POL3* gene is toxic in many constructs in *Escherichia coli* (R. Chanet, personal communication), which probably accounts for our inability to clone *POL3* on the basis of complementation of the mutant defect.

Plasmid LMδ1 was designed to allow replacement of the wild-type copy of *POL3* at the endogenous locus by the *pol3-ct* allele. The 3′ end of the *POL3* gene was amplified from a *pol3-ct* strain using primers p2862 (TAGTAGGAATTCTTGCT TCTGTCCGTCGTGA) and pR4173 (TAGAAGTCGACTAGC GCCCGAAGTCCTCACA). p2862 anneals starting at position +2503 within *POL3*, while pR4173 anneals downstream of *POL3*. The amplified fragment is 1311 bp in length. Underlined nucleotides within primers indicate restriction sites for *Eco*RI (p2862) and *Sal*I (pR4173) that have been added at the 5′ end of the primers to clone the amplified fragment into plasmid pRS306 (New England Biolabs, Beverly, MA) treated with *Eco*RI and *Sal*I. The *Hin*dIII site used for targeting is located 260 bp from the *Sal*I site.

All phenotypic characterizations of *pol3-ct* were performed in the AS strain background except for mitotic prototroph formation, which was assayed in both AS strains and strain BR2495 (Rockmill and Roeder 1990) and its *pol3-ct* derivative LMR1/2. BR2495 has the following genotype: *MAT***a**/*MAT*α *his4-280/his4-260 leu2-27/leu2-3,112 arg4-8/ARG4 thr1-1/thr1-4 cyh10/CYH10 ade2-1/ade2-1 ura3-1/ura3-1 trp1-1/trp1-289*.

Forward mutation, mitotic recombination, and irradiation assays: Forward mutation to canavanine resistance and mitotic intragenic recombination were determined by fluctuation tests using the method of the median. Rates reported are the average of three (30°) or two (18°) independent experiments, each performed with nine independent 5-ml cultures set up from 2-day-old colonies and incubated at 30° or 18°.

Cells in stationary phase (UV) or exponentially growing (γ-rays) were washed in 0.9% NaCl and plated at appropriate dilutions on YPD and synthetic medium. UV irradiation was performed using a 264-nm source delivering 1 J/m^2/sec. γ irradiation was performed using a ^{137}Cs source. Cells were treated with 0, 100, 200, and 400 Gy. Survival was determined as the number of cells forming colonies on YPD medium after a given dose of irradiation divided by the number of colonies derived from cells not irradiated. Each experiment was carried out at least three times with qualitatively similar results.

Genetic analysis: For meiotic analysis of AS strains, cells were incubated in 5 ml of liquid YPD medium overnight, washed once with water, and then resuspended in 10 ml liquid sporulation medium and incubated at 18° for 5 days. Tetrads were treated with zymolyase in 1 M sorbitol for 10 min and dissected on YPAD plates. After 3 days, they were replica plated to appropriate omission media to follow the segregation of nutritive markers. Data were used from four-spore-viable tetrads only, which composed ~60% of tetrads for both wild-type and *pol3-ct* strains. To compare nonparental ditype (NPD) ratios between wild-type and *pol3-ct* strains, a contingency chi-square test was performed for each interval, using the observed and expected NPD values for wild type and mutant.

RESULTS

Isolation and genetic mapping of the *pol3-ct* mutant: A novel screen for mutants defective in meiotic gene conversion was devised. The starting strain is a *HO* diploid homozygous for the *ura3-1* allele at the *URA3* locus on chromosome *V* and for a *ura3-Stu* mutation inserted at the *HIS4* locus on chromosome *III*. This strain was sporulated, and the spores were mutagenized with UV light to 50% survival. Due to mating-type switching followed by mating between cells of opposite mating type, the cells in spore colonies are diploid and homozygous at all loci except *MAT*. Since any newly induced mutations are homozygous, recessive mutations can be readily detected. The diploids still carry *ura3-1* and *ura3-Stu* alleles and thus can be assayed for meiotic gene conversion by screening for the production of Ura^+ prototrophs. A conversion-defective mutant that showed a 10-fold reduction in Ura^+ prototrophs was chosen for further study.

Attempts to clone the gene from a yeast genomic library by complementation of the conversion defect proved unsuccessful. We therefore mapped the gene by tetrad analysis. The mutant was crossed to *ura3-1* strains carrying 48 different markers dispersed throughout the yeast genome (Figure 2). Haploid segregants were scored for a defect in meiotic gene conversion by mating to tester strains carrying *ura3-Stu* and the conversion-defective allele; the resulting diploids were sporulated and screened for the production of uracil prototrophs. This mapping localized the mutation to the left arm of chromosome *IV*, 22 cM centromere proximal to *MSH5* and 30 cM distal to *MBP1*.

In the region defined by mapping, the *POL3* gene, which encodes the catalytic subunit of DNA polymerase δ (Polδ), was the only obvious candidate for the mutated gene. Consistent with this possibility, a plasmid carrying a wild-type copy of *POL3* complements the mutant defect. When the *POL3* gene was amplified from the mu-

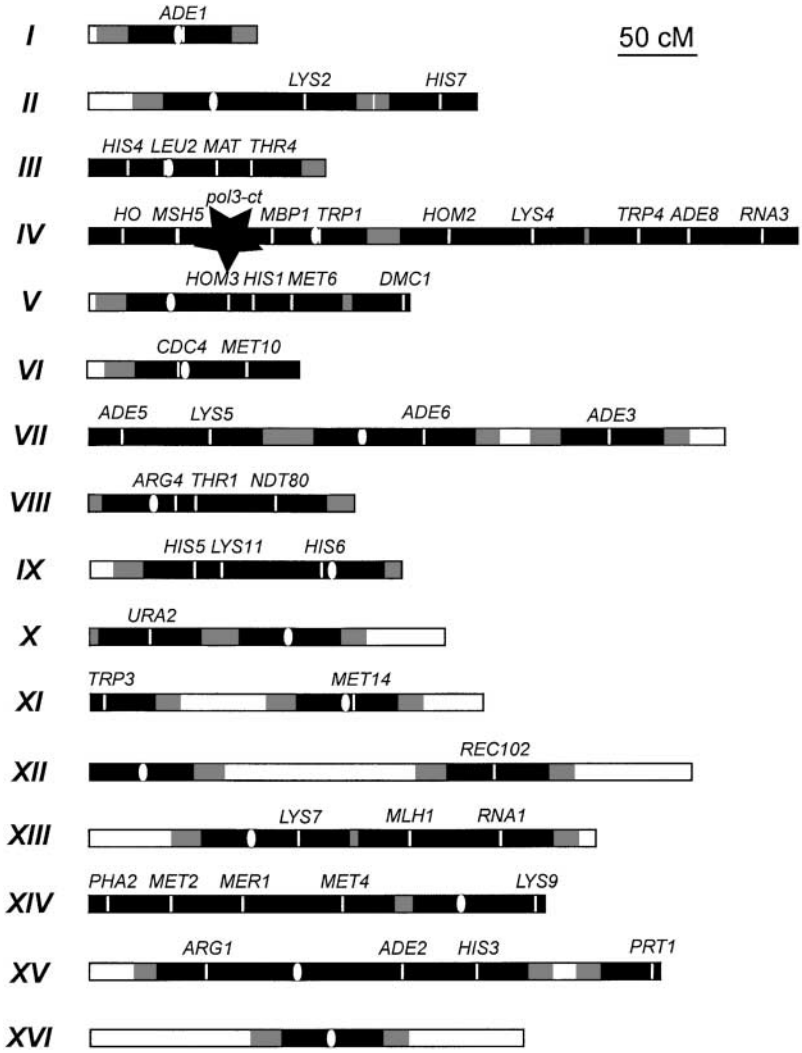

FIGURE 2.—Mapping of conversion-defective mutant. A genetic map showing the 16 chromosomes of yeast is diagrammed. Centromeres are represented by white ovals. The *pol3-ct* mutation was mapped by crossing to strains carrying 48 different markers dispersed throughout the genome. Beyond a genetic distance of 50 cM, genetic independence is expected. Therefore, tetrad analyses showing no linkage between the mutation of interest and a given marker define a region of 50 cM on both sides of the marker in which the mutation cannot lie. Such regions are indicated by rectangles, shown in black up to 35 cM away from the marker and in gray from 35 cM to 50 cM (*e.g.*, the *ADE3* marker on chromosome *VII*). Centromeric markers (*e.g.*, *ADE1* and *TRP1*) indicated that the conversion-defective mutation is not linked to its centromere; therefore, all centromeres are covered by rectangles. Mapping showed that the *pol3-ct* mutation is approximately at the center of a region defined by the *MSH5* and *MBP1* genes.

tant strain by PCR and sequenced, a point mutation was found in the *POL3* open reading frame at position +3268, 11 bp before the last nucleotide (Figure 3A). This allele changes a leucine codon (TTA) to a stop codon (TAA). As a consequence, the protein is missing the last four amino acids (LSKW). The mutant was therefore named *pol3-ct*, for *POL3 C*-terminal *t*runcation. The mutation does not lie in any of the conserved domains of the protein; in particular, *pol3-ct* does not affect the putative zinc finger domains also located near the carboxy terminus of the protein.

***pol3-ct* does not show growth or DNA repair defects:** Since *POL3* is an essential gene responsible for the polymerase and proofreading activities of Polδ (HINDGES and HUBSCHER 1997), it was important to determine the effects of *pol3-ct* in vegetative cells. Growth of *pol3-ct* mutants is normal at 18° and 30°; *pol3-ct* grows slightly slower than wild type at 37° (doubling time of 150 min for *POL3 vs.* 165 min for *pol3-ct*). These results indicate that DNA synthesis is not impaired in *pol3-ct* mutants as it is in thermosensitive mutants of *POL3* that show cell cycle arrest when switched to nonpermissive temperatures (CONRAD and NEWLON 1983).

Replication defects caused by a deficient Polδ can result in the accumulation of mutations (DATTA *et al.* 2000) and/or DNA lesions that are potential recombination substrates (AGUILERA and KLEIN 1988). In addition, Polδ has been proposed to play a role in DNA damage repair (GIOT *et al.* 1997). We therefore examined the effect of *pol3-ct* on mutation rate, mitotic recombination, and sensitivity to DNA-damaging agents. These experiments were carried out at 30°, the optimum temperature for yeast cell growth. In addition, since the meiotic experiments described below were carried out at 18°, a subset of vegetative phenotypes was also examined at this temperature. We found no change in mutation rate at the *CAN1* locus at 30° and a modest (but statistically significant) twofold increase at 18° (Figure 3B). There was no change in mitotic intragenic recombination at either temperature (Figure 3, C and D). The *pol3-ct* mutant does not display enhanced sensitivity to UV irradiation (Figure 3, E and F) or to γ irradiation (Figure 3G).

***pol3-ct* changes the conversion gradient at *HIS4*:** The *pol3-ct* allele was originally found to decrease meiotic intragenic recombination between heteroalleles of the *URA3* gene, suggesting that *pol3-ct* affects gene conver-

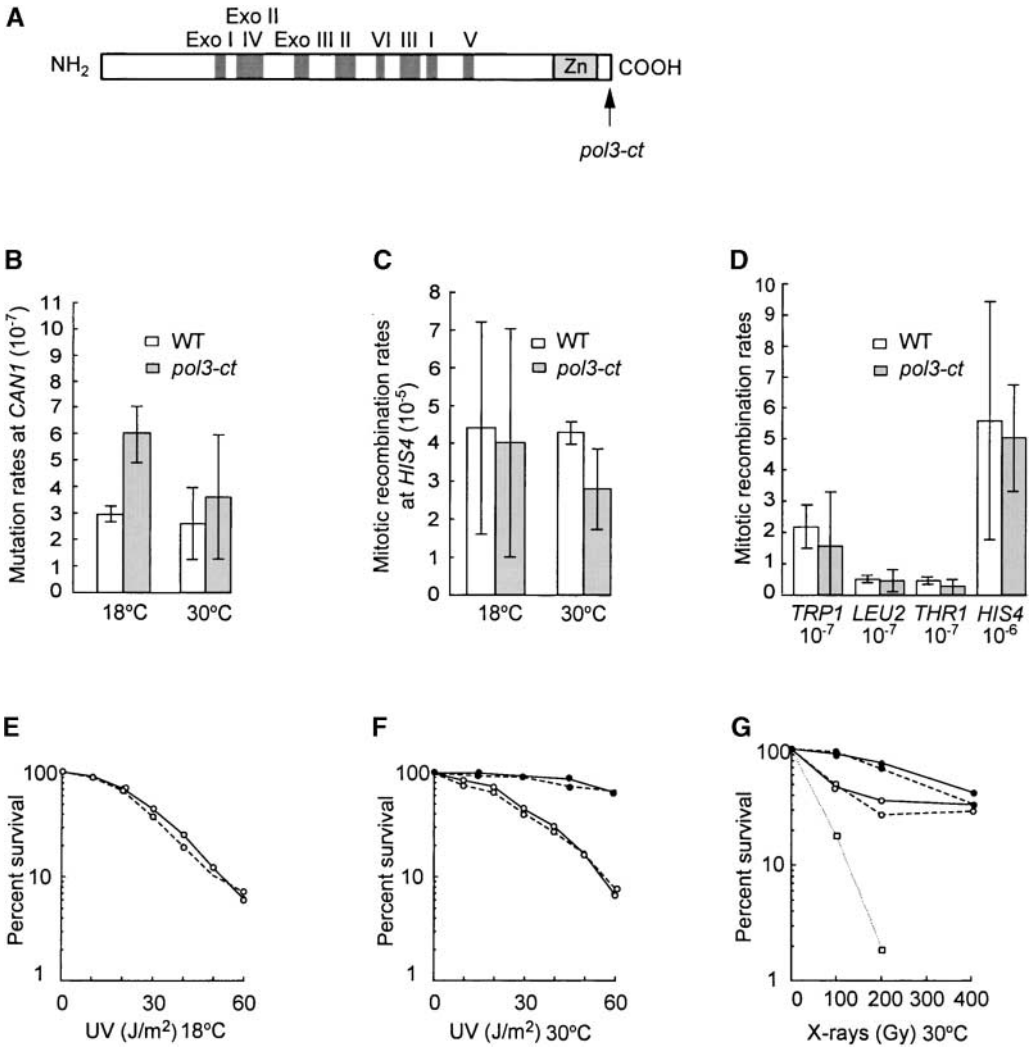

FIGURE 3.—Characterization of *pol3-ct* mutant. (A) Pol3 protein and location of the *pol3-ct* mutation. The coding sequence includes six regions involved in polymerase activity (domains I–VI, shaded), three regions corresponding to the exonuclease proofreading active site (Exo I, II, and III, shaded; Exo II is contained within domain IV), and a putative zinc finger DNA-binding domain (Zn; HINDGES and HUBSCHER 1997). The position of the *pol3-ct* mutation is indicated by an arrow. (B) Mutation rates at the *CAN1* locus determined at 18° and 30°. (C) Mitotic intragenic recombination rates between *HIS4* heteroalleles determined at 18° and 30°. (D) Mitotic intragenic recombination rates at 30° determined in strain BR2495 carrying heteroalleles at four different loci. Error bars in B–D represent standard deviations. (E and F) Sensitivity to UV light at 18° and at 30°. (G) Sensitivity to γ irradiation at 30°. In E–G, solid circles represent diploid strains, and open circles indicate haploid strains; solid lines represent wild-type strains, and dashed lines represent *pol3-ct* strains. A *rad52* haploid, known to be highly sensitive to γ-rays, was used as a control (square symbols).

sion. To determine which step(s) of meiotic gene conversion might be altered, conversion was examined at the *HIS4* recombination hotspot (NAG *et al.* 1989). These experiments were carried out at 18°, the temperature at which the frequency of non-Mendelian segregation is maximal in the strain background used for this analysis.

Non-Mendelian segregation is observed at high frequency at *HIS4* (Table 1) due to the presence of a meiotic DSB site just upstream of the gene (FAN *et al.* 1995). hDNAs spanning regions of heterologies within *HIS4* contain mismatches. Correction of these mismatches can lead to gene conversion (3:1 or 1:3 segregations), whereas unrepaired mismatches lead to postmeiotic segregations (sectored colonies). An important feature of the *HIS4* meiotic hotspot is that it shows a conversion gradient with its high end at the 5′ end of the gene next to the initiation site (DETLOFF *et al.* 1992).

Remarkably, the conversion gradient within *HIS4* is strongly accentuated in the *pol3-ct* background (Table 1; Figure 4A). No effect on non-Mendelian segregation frequencies was seen for the most 5′ marker, indicating that initiation of recombination at *HIS4* is not altered in a *pol3-ct* background. In contrast, there is a decrease in gene conversion for all other markers in *HIS4*. The effect of *pol3-ct* increases progressively within *HIS4* to a maximum of sixfold at the 3′ end of the gene. We therefore conclude that formation of hDNAs starting at the initiation site upstream of *HIS4* is not impaired in the *pol3-ct* mutant. However, these hDNAs extend shorter distances into *HIS4* in *pol3-ct* than in wild type.

Previous studies have shown that polarity gradients are largely abolished when mismatch repair is inhibited (DETLOFF *et al.* 1992; ALANI *et al.* 1994). Two observations indicate that the effect of *pol3-ct* on the *HIS4* conversion gradient is not due to an alteration in the efficiency of mismatch repair. First, for none of the *his4*

TABLE 1

Effect of the *pol3-ct* mutation on non-Mendelian segregation frequencies of heterozygous markers

Diploid strain	Marker	Position in *HIS4*	*POL3*	Segregation pattern 4:4	6:2	2:6	5:3	3:5	ab4:4	8:0	0:8	Other	Total tetrads	% NMS	Fold decrease
AS4/PD75	*his4-ACG*	+2	wt	251	88	98	5	5	0	6	10	0	463	45.7	
LMP6/LMP5	*his4-ACG*	+2	*pol3-ct*	243	80	95	0	0	0	8	4	0	430	43.6	1.0
AS4/PD5	*his4-519*	+473	wt	296	53	65	0	0	0	3	1	0	425	30.3	
LMP6/LMP2	*his4-519*	+473	*pol3-ct*	376	33	38	0	0	0	1	1	0	449	16.2	1.9*
AS4/PD22	*his4-712*	+1396	wt	378	33	70	0	0	0	1	1	0	483	21.7	
LMP6/LMP3	*his4-712*	+1396	*pol3-ct*	458	9	14	0	0	0	0	0	0	481	4.8	4.5*
AS4/PD24	*his4-713*	+2270	wt	388	19	44	1	0	0	1	0	0	452	14.1	
LMP6/LMP4	*his4-713*	+2270	*pol3-ct*	344	1	7	0	0	0	0	0	0	352	2.3	6.1*
AS4/DNY25	*his4-lopc*	+473	wt	247	41	11	62	45	12	1	0	5	425	41.9	
LMP6/LMP8	*his4-lopc*	+473	*pol3-ct*	360	28	4	16	20	3	0	0	1	432	16.6	2.5*
AS/PD	*arg4-17*		wt	2062	101	85	0	0	0	1	2	0	2248	8.4	
LMP/LMP	*arg4-17*		*pol3-ct*	2076	35	33	0	0	0	0	0	0	2144	3.1	2.7*
AS/PD	*tyr7-1*		wt	975	17	25	6	0	0	1	0	0	1024	4.8	
LMP/LMP	*tyr7-1*		*pol3-ct*	1210	10	19	1	0	0	0	0	0	1240	2.4	2.0*
AS/PD	*leu2-Bst*		wt	2184	21	43	0	0	0	0	0	0	2248	2.8	
LMP/LMP	*leu2-Bst*		*pol3-ct*	2079	24	41	0	0	0	0	0	0	2144	3.0	1.0
AS/PD	*MAT*		wt	2197	27	24	0	0	0	0	0	0	2248	2.3	
LMP/LMP	*MAT*		*pol3-ct*	2136	6	2	0	0	0	0	0	0	2144	0.4	5.7*

Diploid strains are designated according to the names of their haploid parents (see MATERIALS AND METHODS). Data for the *ARG4*, *TYR7*, *LEU2*, and *MAT* markers represent pooled data from the five wild-type strains and the five *pol3-ct* strains used to examine the segregation of different *HIS4* alleles. wt, *POL3/POL3* diploid; *pol3-ct*, *pol3-ct/pol3-ct* diploid. The nomenclature used for meiotic segregation frequencies refers to the eight DNA strands (four chromatids) present in meiotic prophase. The different types of meiotic segregation are 4:4 (normal Mendelian segregation), 6:2 and 2:6 (gene conversion), 5:3 and 3:5 (tetrads with one sectored colony indicating an unrepaired mismatch in hDNA), ab4:4 (aberrant 4:4; one wild-type, one mutant, and two sectored colonies), and 8:0 and 0:8 (tetrads with four spores of a single genotype). "Other" includes aberrant 6:2 segregations (two wild-type and two sectored colonies) and aberrant 2:6 segregations (two mutant and two sectored colonies) as well as 7:1 segregations (one sectored and three wild-type colonies) and 1:7 (one sectored and three mutant colonies). The percentages of non-Mendelian segregation in wild-type and *pol3-ct* strains were compared by chi-square tests. *Fold decreases from wild type that are statistically significant ($P < 0.001$). NMS, non-Mendelian segregation.

alleles examined does the *pol3-ct* mutation increase the frequency of 5:3 and 3:5 segregations (indicative of a failure to repair) relative to 6:2 and 2:6 segregations (indicative of repair). Second, a *HIS4* mutation (*his4-lopc*) that usually escapes mismatch repair (even in wild type) shows a decreased frequency of non-Mendelian segregation in the *pol3-ct* mutant (Table 1).

The *pol3-ct* effect on gene conversion is not specific to the *HIS4* locus: The decrease in meiotic gene conversion in *pol3-ct* is not specific to *HIS4*. A twofold decrease in conversion was also found at the *ARG4* and *TYR7* loci (Table 1). At the *MAT* locus, parental alleles in diploids differ by a heterology of 700 bp. An *mlh1* mutant, which is deficient in mismatch repair, shows high frequencies

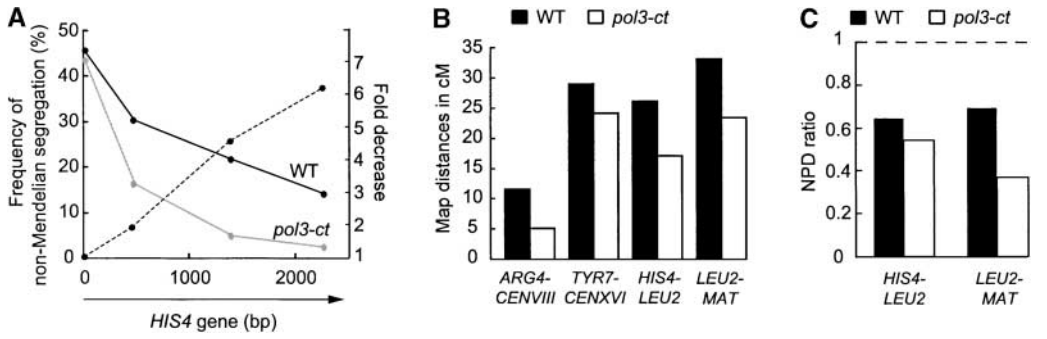

FIGURE 4.—Gene conversion, crossing over, and crossover interference in the *pol3-ct* mutant. (A) The solid lines indicate the frequency of non-Mendelian segregation at different positions in *HIS4* for wild-type and *pol3-ct* strains. The dashed line indicates the fold decrease in non-Mendelian segregation frequency in *pol3-ct* compared to wild type. The graph is derived from the data in Table 1. (B) Map distances in centimorgans for four different intervals in wild type and *pol3-ct*. (C) Crossover interference in the *HIS4-LEU2* and *LEU2-MAT* intervals. The dashed line indicates the NPD value expected in the absence of interference. Histograms in B and C are derived from the data in Table 2.

TABLE 2

Effect of the *pol3-ct* mutation on map distances and NPD ratios

Interval	Genotype	PD	NPD	TT	cM	% wt	Prob.	NPD exp.	NPD ratio	Prob.
HIS4-LEU2	*POL3*	866	29	615	26.1			45	0.64	<0.02
HIS4-LEU2	*pol3-ct*	1197	13	512	17.1	65	<0.001	24	0.54	<0.05
LEU2-MAT	*POL3*	1038	66	1006	33.2			95	0.69	<0.01
LEU2-MAT	*pol3-ct*	1210	22	835	23.4	70	<0.001	60	0.37	<0.001

Interval	Genotype	PD + NPD	TT	cM	% wt	Prob.
ARG4-CENVIII	*POL3*	1552	470	11.6		
ARG4-CENVIII	*pol3-ct*	1721	196	5.1	44	<0.001
TYR7-CENXVI	*POL3*	409	565	29		
TYR7-CENXVI	*pol3-ct*	623	587	24.2	83	<0.001

For each interval, the size of the map distance as a percentage of the map distance in wild type (% wt) is indicated. Also presented is the probability (Prob.), based on a chi-square test, that the difference between wild-type and mutant map distances is due to chance. For the *HIS4-LEU2* and *LEU2-MAT* intervals, map distances were calculated using the following formula: map distance (in centimorgans) = [(TT + 6NPD)/2(PD + NPD + TT)] × 100. The number of NPD tetrads expected (NPD exp.) in the absence of interference was calculated on the basis of the observed number of TT tetrads (Papazian 1952). The NPD ratio is the number of NPD tetrads observed divided by the number expected. The probability (Prob.), based on a chi-square test, that the difference between the observed and expected numbers of NPD tetrads is due to chance is indicated. Map distance between *ARG4* (or *TYR7*) and its centromere was determined using a *trp1* mutation, which is tightly linked to its centromere on chromosome *IV*. In this case, map distances were calculated using the following formula: map distance (in centimorgans) = [½TT/(PD + NPD + TT)] × 100. PD, parental ditype; NPD, nonparental ditype; TT, tetratype.

of postmeiotic segregation at *MAT*, indicating formation of hDNA with large loops at this locus (Wang *et al.* 1999). Conversion of this heterology is decreased sixfold in *pol3-ct* (Table 1), strengthening the conclusion that the decrease in gene conversion does not depend on the nature of the segregating mutations. No decrease in conversion was observed for the *leu2-Bst* marker. On the basis of the results obtained at *HIS4*, it is likely that the *leu2-Bst* marker is close to a recombination initiation site.

Crossing over is decreased in *pol3-ct* strains: *pol3-ct* strains show wild-type levels of sporulation (~30%) and spore viability (~90%). These results, together with the studies of gene conversion described above, indicate that DSB formation and repair occur as efficiently in *pol3-ct* strains as they do in wild type. To gain insight into the resolution of recombination intermediates in the mutant, crossover formation was analyzed by measuring map distances in four genetic intervals on three different chromosomes. In all intervals, map distances are decreased, on average to 66% of the wild-type level (Table 2; Figure 4B). These results suggest a role for DNA synthesis in promoting crossover formation.

Crossovers show interference in *pol3-ct* strains: Meiotic crossovers are nonrandomly distributed such that two crossovers rarely occur close together, a phenomenon known as crossover interference. The effect of the *pol3-ct* mutation on interference was investigated by measuring NPD ratios, which can be roughly defined as the frequency of double crossovers observed in a marked interval divided by the number expected in the absence of interference (Papazian 1952; Snow 1979). An NPD ratio of <1.0 indicates positive interference. Crossover interference is not decreased in the *pol3-ct* mutant (Table 2; Figure 4C). In fact, in both intervals tested, the NPD ratio in the mutant is lower than that in wild type (indicating stronger interference); this difference is statistically significant only in the *LEU2-MAT* interval ($P < 0.05$).

DISCUSSION

***pol3-ct* is a separation-of-function allele:** Previous studies of the role of Polδ in recombination have been complicated by the use of temperature-sensitive alleles, which have modest defects in DNA replication even at permissive temperatures. Nevertheless, it has been possible to show that Polδ is required in vegetative cells for gene conversion events induced by irradiation and for repair of a DSB at the *MAT* locus (Fabre *et al.* 1991; Holmes and Haber 1999). This study is the first to demonstrate a role for Polδ in meiotic recombination. Our data demonstrate that the *pol3-ct* mutant has little or no defect in DNA replication or DNA damage repair in vegetative cells. In addition, we have found that *pol3-ct* does not affect spore formation or spore viability, indicating that premeiotic DNA replication is efficient. Thus, *pol3-ct* acts as a separation-of-function allele that specifically impairs a function of Polδ involved in meiotic recombination. This characteristic of the *pol3-ct* allele makes it a unique tool to investigate the role of Polδ

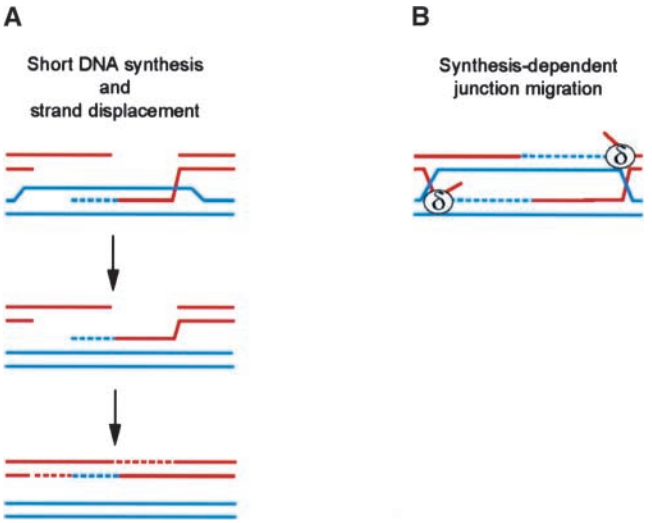

FIGURE 5.—Models for the effect of the *pol3-ct* mutation on meiotic recombination. (A) Proposed effect of *pol3-ct* in the SDSA pathway. (B) Proposed effect of *pol3-ct* on the DSB repair pathway. See text for explanation.

in meiotic recombination, unimpeded by the complications associated with temperature-sensitive mutations.

Possible roles for Polδ in determining gene conversion tract length: Our results suggest that *pol3-ct* strains initiate the wild-type number of meiotic recombination events; however, the average length of hDNA formed is shorter than that in wild type. It is not clear why the *pol3-ct* mutation was originally identified on the basis of decreased prototroph formation between *URA3* heteroalleles. Perhaps both *URA3* alleles are far from a DSB site; in this case, shortening tract length might decrease the fraction of events that reach either mutation.

What does the decrease in gene conversion tract length in *pol3-ct* strains tell us about the role of wild-type Polδ in meiotic recombination? Recombination events channeled through the DSB repair pathway necessitate the synthesis of new DNA sufficient to replace the sequences removed by processing of DSBs to expose single-stranded tails (Figure 1, left). Therefore, in this pathway, the length of asymmetric hDNA should be at least equivalent to the lengths of the single-stranded tails present at DSB sites. In contrast, in the SDSA pathway, displacement of the invading strand might occur before DNA synthesis extends the full length of the single-stranded tail on the other side of the DSB site (Figure 5A). In this case, repair synthesis would have to be completed after annealing of the displaced strand to the complementary single strand. The length of hDNA would then be confined to the length of DNA synthesis that occurred on the invaded chromatid. In the *pol3-ct* mutant, DNA repair synthesis might frequently stop earlier than in wild type, perhaps due to weakened processivity of Polδ during recombination.

How might the *pol3-ct* mutation affect tract length for gene conversion events that proceed through the DSB repair pathway? We propose a model in which Polδ does not simply serve to fill in single-stranded gaps, but rather plays a determining role in hDNA extension. According to the DSB repair model, DNA synthesis primed from the 3′ end of the invading strand enlarges the D-loop; the displaced DNA subsequently captures the second single-stranded tail, which in turn primes repair synthesis. We propose that Polδ subsequently increases the length of asymmetric hDNA by promoting DNA synthesis that is coupled to extended removal of the resected strand either by strand displacement or by further 5′ to 3′ resection (Figure 5B). In this scenario, DNA synthesis would be *de facto* coupled with junction migration; consequently, asymmetric hDNA could be extended prior to the formation of ligated double Holliday junctions. This hypothesis would explain nicely why asymmetric hDNAs at *HIS4* (and at other recombination hotspots such as *ARG4* and *CYS3*) frequently span the entire gene while the initial single-stranded tails appear to be no longer than 800 nucleotides (SUN *et al.* 1991; BISHOP *et al.* 1992; DETLOFF and PETES 1992; VEDEL and NICOLAS 1999).

A specific interaction between Polδ and a component of the recombination apparatus might be required for synthesis-coupled junction migration. In the *pol3-ct* mutant, this interaction might not occur efficiently such that Polδ is removed upon reaching the first 5′ end, thus preventing further hDNA extension.

Possible roles for Polδ in meiotic crossing over: In addition to altering the length of gene conversion tracts, *pol3-ct* also decreases the frequency of crossing over. How can this observation be reconciled with the models just presented (Figure 5)?

If single-end invasion intermediates sustain shorter tracts of DNA synthesis in *pol3-ct* (Figure 5B), this would facilitate strand displacement and favor the repair of DSBs through the SDSA pathway. Since SDSA is not associated with crossing over, a bias toward SDSA (*vs.* the DSB repair pathway) could account for the decrease in crossing in *pol3-ct* strains.

An alternative (not mutually exclusive) possibility is that *pol3-ct* decreases the probability of crossing over for events that proceed through the DSB repair pathway. Polδ might be involved in isomerization and/or the decision as to which strands are to be cut during Holliday junction resolution. For example, the resolvase that introduces nicks into strands of like polarity at Holliday junctions could be directed by Polδ to operate on strands with newly synthesized DNA. Such a bias would favor cutting the two junctions in opposite directions and thereby encourage crossover formation. Premature removal of Polδ would mean loss of the bias and a decrease in crossing over.

***pol3-ct* does not impair crossover interference:** A number of mutants (*e.g.*, *zip1*, *msh4*) show a two- to threefold decrease in crossing over that is not associated with decreased initiation of recombination (SYM and ROEDER

1994; Novak *et al.* 2001). These mutations also eliminate crossover interference. The *pol3-ct* mutation reduces crossing over without decreasing interference, raising the possibility that *pol3-ct* affects a different subset of crossovers from those eliminated by *zip1* and *msh4*. The fact that interference appears slightly stronger in the *pol3-ct* mutant raises the possibility that *pol3-ct* specifically (or preferentially) reduces a subset of crossovers that do not normally exhibit interference. The existence of two crossover pathways, one subject to interference and the other free of interference, is consistent with recent observations (de los Santos *et al.* 2003).

Meiotic crossovers are nonrandomly distributed among chromosomes, such that every chromosome pair almost always undergoes at least one crossover (an obligate crossover) to ensure its correct segregation at meiosis I. Crossover interference and obligate crossing over are often assumed to be mechanistically related. Consistent with this hypothesis, mutations that decrease crossover interference also reduce spore viability due to the missegregation of nonrecombinant chromosomes (Sym and Roeder 1994; Chua and Roeder 1997; Novak *et al.* 2001). The wild-type level of spore viability observed in *pol3-ct* strains suggests that crossovers are properly distributed among chromosomes.

The *pol3-ct* mutation links replication and recombination: Further studies using the *pol3-ct* mutant will lead to a better understanding of the mechanism by which Polδ influences gene conversion tract length and crossing over. This study casts new light on our growing awareness of the links between DNA replication and homologous recombination. It is now generally acknowledged that homologous recombination serves as a backup system supporting DNA replication when the template DNA is damaged or the replication machinery malfunctions (Kuzminov 2001). It is fascinating to unveil, on the other hand, that the outcome of homologous recombination depends largely on a major DNA replication protein.

We thank Roland Chanet and Tom Petes for kindly providing plasmids and yeast strains. L.M. especially thanks Eun-Jin Erica Hong for valuable comments on the manuscript and Michael Odell, Roberta Shew, and Nadia Shapiro for excellent technical assistance. This work was supported by the Howard Hughes Medical Institute, le Commissariat à l'Energie Atomique, and Electricité de France. L.M. was supported by postdoctoral fellowships from the Association pour la Recherche sur le Cancer and from the European Molecular Biology Organization.

LITERATURE CITED

Aguilera, A., and H. L. Klein, 1988 Genetic control of intrachromosomal recombination in *Saccharomyces cerevisiae*. Isolation and genetic characterization of hyper-recombination mutations. Genetics **119:** 779–790.

Alani, E., R. A. G. Reenan and R. D. Kolodner, 1994 Interaction between mismatch repair and genetic recombination in *Saccharomyces cerevisiae*. Genetics **137:** 19–39.

Allers, T., and M. Lichten, 2001 Differential timing and control of noncrossover and crossover recombination during meiosis. Cell **106:** 47–57.

Bishop, D. K., D. Park, L. Xu and N. Kleckner, 1992 *DMC1*: a meiosis-specific yeast homolog of E. coli *recA* required for recombination, synaptonemal complex formation, and cell cycle progression. Cell **69:** 439–456.

Chua, P. R., and G. S. Roeder, 1997 Tam1, a telomere-associated meiotic protein, functions in chromosome synapsis and crossover interference. Genes Dev. **11:** 1786–1800.

Conrad, M. N., and C. S. Newlon, 1983 *Saccharomyces cerevisiae cdc2* mutant fails to replicate approximately one-third of their nuclear genome. Mol. Cell. Biol. **3:** 1000–1012.

Datta, A., J. L. Schmeits, N. S. Amin, P. J. Lau, K. Muyung *et al.*, 2000 Checkpoint-dependent activation of mutagenic repair in *Saccharomyces cerevisiae pol3-01* mutants. Mol. Cell **6:** 593–603.

de los Santos, T., N. Hunter, C. Lee, B. Larkin, J. Loidl *et al.*, 2003 The Mus81/Mms4 endonuclease acts independently of double-Holliday junction resolution to promote a distinct subset of crossovers during meiosis in budding yeast. Genetics **164:** 81–94.

Detloff, P., and T. D. Petes, 1992 Measurements of excision repair tracts formed during meiotic recombination in *Saccharomyces cerevisiae*. Mol. Cell. Biol. **12:** 1805–1814.

Detloff, P., M. A. White and T. D. Petes, 1992 Analysis of a gene conversion gradient at the *HIS4* locus in *Saccharomyces cerevisiae*. Genetics **132:** 113–123.

Fabre, F., A. Boulet and G. Faye, 1991 Possible involvement of the yeast POLIII DNA polymerase in induced gene conversion. Mol. Gen. Genet. **229:** 353–356.

Fan, Q., F. Xu and T. D. Petes, 1995 Meiosis-specific double-strand DNA breaks at the *HIS4* recombination hotspot in the yeast *Saccharomyces cerevisiae*: control in *cis* and *trans*. Mol. Cell. Biol. **15:** 1679–1688.

Giot, L., R. Chanet, M. Simon, C. Facca and G. Faye, 1997 Involvement of the yeast DNA polymerase δ in DNA repair *in vivo*. Genetics **145:** 1239–1251.

Hindges, R., and U. Hubscher, 1997 DNA polymerase δ, an essential enzyme for DNA transactions. Biol. Chem. **378:** 345–362.

Holmes, A. M., and J. E. Haber, 1999 Double-strand break repair in yeast requires both leading and lagging strand DNA polymerases. Cell **96:** 415–424.

Hunter, N., and N. Kleckner, 2001 The single-end invasion: an asymmetric intermediate at the double-strand break to double-Holliday junction transition of meiotic recombination. Cell **106:** 59–70.

Kuzminov, A., 2001 DNA replication meets genetic exchange: chromosomal damage and its repair by homologous recombination. Proc. Natl. Acad. Sci. USA **98:** 8461–8468.

Merker, J. D., M. Dominska and T. D. Petes, 2003 Patterns of heteroduplex formation associated with the initiation of meiotic recombination in the yeast *Saccharomyces cerevisiae*. Genetics **165:** 47–63.

Nag, D. K., M. A. White and T. D. Petes, 1989 Palindromic sequences in heteroduplex repair in yeast. Nature **340:** 318–320.

Novak, J. E., P. Ross-Macdonald and G. S. Roeder, 2001 The budding yeast Msh4 protein functions in chromosome synapsis and the regulation of crossover distribution. Genetics **158:** 1013–1025.

Papazian, H. P., 1952 The analysis of tetrad data. Genetics **37:** 175–188.

Paques, F., and J. E. Haber, 1999 Multiple pathways of recombination induced by double-strand breaks in *Saccharomyces cerevisiae*. Microbiol. Mol. Biol. Rev. **63:** 349–404.

Rockmill, B., and G. S. Roeder, 1990 Meiosis in asynaptic yeast. Genetics **126:** 563–574.

Rockmill, B., E. J. Lambie and G. S. Roeder, 1991 Spore enrichment. Methods Enzymol. **194:** 146–149.

Rothstein, R., 1991 Targeting, disruption, replacement and allele rescue: integrative DNA transformation in yeast. Methods Enzymol. **194:** 281–301.

Snow, R., 1979 Maximum likelihood estimation of linkage and interference from tetrad data. Genetics **92:** 231–245.

Sun, H., D. Treco, N. P. Schultes and J. W. Szostak, 1989 Double-strand breaks at an initiation site for meiotic gene conversion. Nature **338:** 87–90.

Sun, H., D. Treco and J. W. Szostak, 1991 Extensive 3′-overhang-

ing, single-stranded DNA associated with the meiosis-specific double-strand breaks at the *ARG4* recombination initiation site. Cell **64:** 1155–1161.

Sym, M., and G. S. Roeder, 1994 Crossover interference is abolished in the absence of a synaptonemal complex protein. Cell **79:** 283–292.

Szostak, J. W., T. L. Orr-Weaver, R. J. Rothstein and F. W. Stahl, 1983 The double-strand-break repair model for recombination. Cell **33:** 25–35.

Vedel, M., and A. Nicolas, 1999 *CYS3*, a hotspot of meiotic recombination in *Saccharomyces cerevisiae*: effects of heterozygosity and mismatch repair functions on gene conversion and recombination intermediates. Genetics **151:** 1245–1259.

Wang, T.-F., N. Kleckner and N. Hunter, 1999 Functional specificity of MutL homologs in yeast: evidence for three Mlh1-based heterocomplexes with distinct roles during meiosis in recombination and mismatch correction. Proc. Natl. Acad. Sci. USA **96:** 13914–13919.

Communicating editor: L. S. Symington